DALTON
FULL PAPER

Oxidatively induced M–C bond cleavage reactions of $Cp^*Ir(Me_2SO)Me_2$ and $Cp^*Rh(Me_2SO)Me_2$ ($Cp^* = \eta^5$-C_5Me_5) †

Erik Fooladi,[a] Todd Graham,[b] Michael L. Turner,[b] Bjørn Dalhus,[a] Peter M. Maitlis *[b] and Mats Tilset *[a]

[a] *Department of Chemistry, University of Oslo, P.O. Box 1033 Blindern, N-0315 Oslo, Norway. E-mail: mats.tilset@kjemi.uio.no*
[b] *Department of Chemistry, University of Sheffield, Sheffield, UK S3 7HF. E-mail: P. Maitlis@sheffield.ac.uk*

Received 16th August 2001, Accepted 14th November 2001
First published as an Advance Article on the web 13th February 2002

Electrochemical and chemical oxidation of $Cp^*Ir(Me_2SO)Me_2$ (**1**; $Cp^* = \eta^5$-C_5Me_5) in Me_2SO lead to the formation of methane and traces of ethene (ratio *ca.* 20 : 1) as well as $Cp^*Ir(Me_2SO)_2Me^+$. Labeling studies indicate that three of the methane hydrogen atoms arise from the iridium-bonded methyl, while the fourth appears to arise from adventitious water. By contrast, oxidation of the rhodium analog $Cp^*Rh(Me_2SO)Me_2$ gave only ethane and $Cp^*Rh(Me_2SO)_2Me^+$. Quantitative derivative cyclic voltammetry (DCV) showed that the disappearance of electrode-generated $\mathbf{1}^{\bullet+}$ follows a rate law that is second order with respect to Ir. The Rh analog $\mathbf{6}^{\bullet+}$ reacted at rates too great to be measured by DCV under these conditions. Possible mechanisms for these reactions are discussed, and particular attention is paid to the reactivity differences between Rh and Ir. Convenient new syntheses of $Cp^*Ir(Me_2SO)Me_2$ and $Cp^*Rh(Me_2SO)Me_2$, as well as X-ray structure determinations of these compounds and of $Cp^*Ir(Me_2SO)_2Me^+$, are reported.

Introduction

Reductive elimination is a fundamentally important process of organometallic reactivity and is often the mechanism by which organic products are liberated from the metal in a catalytic process. Simple intuitive rules of thumb imply that when comparisons are made between related compounds, reductive elimination becomes more facile when the metal center is more electron deficient, for example through increased charge and/or formal oxidation state.[1] Accordingly, it has been frequently demonstrated that the electron-transfer oxidation of organotransition-metal complexes containing σ-bonded ligands may induce reductive elimination reactions. Several distinct mechanisms have been observed for these eliminations, defined in a broad sense as shown in eqns. (1)–(3). Homolytic[2] [eqn. (1)] and concerted reductive elimination [eqn. (2)] processes[2–4] are both found for compounds containing σ-bonded hydrocarbyl ligands. The heterolytic process shown in eqn. (3) is commonly seen for metal hydrides.[5] The facile elimination reactions may be viewed as a consequence of the metal–X bond weakening caused by the one-electron oxidation process.[6]

We have previously reported[3f] a detailed investigation of the kinetics and mechanism for the reductive elimination of ethane from the cation radical of $Cp^*Rh(PPh_3)Me_2$ in acetonitrile.[7] A first-order process resulted in intramolecular ethane formation according to eqn. (2). Solvent coordination and further oxidation yielded the solvento complex $Cp^*Rh(PPh_3)(NCMe)_2^{2+}$ as the first observed Rh-containing product after an overall two-electron process. In a separate experiment, it was shown that $Cp^*Rh(PPh_3)(NCMe)_2^{2+}$ reacts with the substrate to give the comproportionation product $Cp^*Rh(PPh_3)(NCMe)Me^+$, but this reaction was orders of magnitude slower than the initial reductive elimination of ethane from $Cp^*Rh(PPh_3)Me_2^{\bullet+}$.[3f] The oxidation of Cn^*RhMe_3[7] also resulted in unimolecular ethane elimination.[3j] Similarly, oxidation of the stable hydridomethyl complex $Cp^*Ir(PPh_3)(H)Me$ initiated the elimination of methane. In contrast, oxidation of the dimethyl complex $Cp^*Ir(PPh_3)Me_2$ resulted in a relatively stable cation radical[3g,8] which eventually reacted to give $Cp^*Ir(PPh_3)(NCMe)Me^+$ and CH_4 in acetonitrile. The fourth hydrogen atom in CH_4 was derived from the Cp* ligand.[3g] Others have also demonstrated that Ir-mediated C–H bond activation occurs at the Cp* ligand of $Cp^*Ir(PPh_3)Me_2^{\bullet+}$.[8] Reductive elimination of ethane occurred only to a minor extent, and these results point at potentially fundamental differences in the reactivities of Rh and Ir complexes.

In this contribution we report the results of an investigation of the oxidation of $Cp^*Ir(Me_2SO)Me_2$ (**1**) and its Rh analog $Cp^*Rh(Me_2SO)Me_2$ (**6**). The Ir compound **1** was first reported by Maitlis and co-workers in 1983 and has since then been shown to exhibit a rich and varied reaction chemistry, including exchange of the Me_2SO ligand with other two-electron donors and C–H activation of certain organic compounds.[9a–f] The Rh complex **6** has also been briefly examined.[9g] In order to shed some further light on reactivity differences between second- and third-row transition metals, we compare the behavior of $Cp^*Ir(Me_2SO)Me_2$ and the Rh analog, as well as some previously studied related complexes.

$$\overset{\bullet+}{M}\!-\!R \longrightarrow M^+ + R^\bullet \quad \text{one-electron, one-ligand reductive elimination (homolysis)} \quad (1)$$

$$\overset{\bullet+}{M}\!\begin{matrix}R\\R'\end{matrix} \longrightarrow \overset{\bullet+}{M} + R\!-\!R \quad \text{two-electron, two-ligand reductive elimination} \quad (2)$$

$$\overset{\bullet+}{M}\!-\!R \longrightarrow M^\bullet + R^+ \quad \text{two-electron, one-ligand reductive elimination} \quad (3)$$

† Dedicated to the memory of John Osborn (1939–2000), outstanding inorganic chemist, superb companion, and generous friend.

Electronic supplementary information (ESI) available: rotatable 3-D crystal structure diagrams in CHIME format. See http://www.rsc.org/suppdata/dt/b1/b107451m/

DOI: 10.1039/b107451m

Results

Electrochemical oxidation of Cp*Ir(Me$_2$SO)Me$_2$ (1) in Me$_2$SO

The oxidation of **1** was investigated by cyclic voltammetry (CV). Fig. 1 shows a cyclic voltammogram recorded in Me$_2$SO/

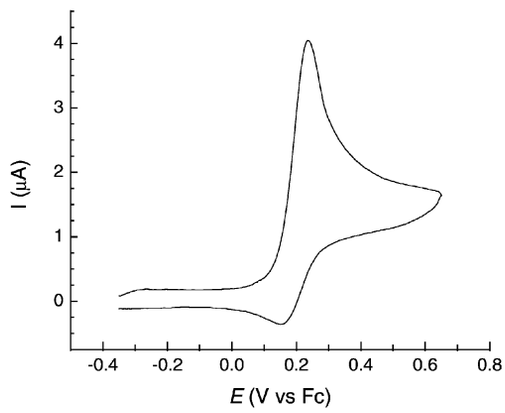

Fig. 1 Cyclic voltammogram of Cp*Ir(Me$_2$SO)Me$_2$ (1.0 mM) in Me$_2$SO/0.1 M $Bu_4N^+PF_6^-$ at a Pt disk electrode (d = 0.6 mm) at 20 °C at voltage scan rate v = 1.0 V s^{-1}.

0.1 M $Bu_4N^+PF_6^-$ (Pt disk electrode, d = 0.6 mm, 20 °C) at a voltage scan rate v of 1.0 V s^{-1}.

As can be seen in the voltammogram, the electrode reaction is partially chemically reversible on the measurement time scale. Voltammograms at variable scan rates revealed that the electrode process approaches chemical reversibility at high scan rates (> 100 V s^{-1}) and is essentially irreversible at low scan rates (< 0.1 V s^{-1}), indicating that subsequent homogeneous reactions consume electrode-generated $\mathbf{1}^{\bullet+}$ on the CV time scale. The reversible electrode potential for the **1**/$\mathbf{1}^{\bullet+}$ couple [$E°_{ox}$(**1**)], taken as the midpoint between the anodic and cathodic peaks at high scan rates, was measured to be +0.18 V *vs.* the Cp_2Fe/Cp_2Fe^+ (Fc) couple. The peak-to-peak separation (ΔE_p) of about 80 mV at v = 1.0 V s^{-1} is somewhat greater than for the Fc couple (ΔE_p = 63 mV under identical conditions and with equal concentrations), indicative of a quasi-reversible electron transfer step. At low scan rates, adsorption at the electrode surface was evident through clear deterioration of the electrode response after repeated cycling. However, with the relatively fast scan rates used for the kinetic measurements described below, no signs of adsorption were discernible. The observed ΔE_p, coulometry data (see below), and the linear dependence of i_p *vs.* $v^{1/2}$ at v = 0.4–20 V s^{-1} [10] are indicative of an overall one-electron transfer process on the CV time scale.[11]

Constant-potential coulometry measurements for the oxidation of **1** were carried out at working electrode potentials 0.10–0.14 V positive of $E°_{ox}$(**1**) on 1.3–1.4 mM substrate solutions in Me$_2$SO/0.05 M $Me_4N^+BF_4^-$.[12] The measurements indicated the consumption of approximately 1 Faraday mol^{-1} for the complete consumption of **1** (n_{obs} = 0.9–1.4 F mol^{-1}).[13] Addition of water (0.2% v/v) to the solution caused no significant difference in the electron transfer stoichiometry (see below). A GC analysis of the vapor phase above the solution after exhaustive electrolysis showed the formation of methane and ethene in an approximate molar ratio of 9 : 1. The only organometallic product that could be detected after work-up was Cp*Ir(Me$_2$SO)$_2$Me$^+$BF$_4^-$ [**2**(BF$_4^-$)], identified by comparison of its ^{1}H NMR spectrum with that of an independently prepared sample (*vide infra*). The product was isolated as a light yellow, air stable solid in greater than 80% yield.

Qualitatively, it was seen that the extent of chemical reversibility of the CV response was dependent on the concentration of **1**, which indicated that the composite reaction-order with respect to $\mathbf{1}^{\bullet+}$ and **1** was greater than unity. This was quantified through an extensive investigation of the kinetics and mechanism of the reaction of $\mathbf{1}^{\bullet+}$ in Me$_2$SO by derivative cyclic voltammetry (DCV). The technique has been described in detail in reviews, and applications of DCV for the investigation of the reactivity of electrode-generated transient organometallic complexes have been reported.[3f,h,j,5e,14] A DCV reaction-order analysis of the oxidation of **1** in Me$_2$SO/0.1 M $Bu_4N^+PF_6^-$ at 25 °C established that the homogeneous reaction that consumes $\mathbf{1}^{\bullet+}$ was cleanly second order over the substrate concentration range 0.5–2.0 mM. The rate law for consumption of $\mathbf{1}^{\bullet+}$ can then be second-order with respect to $\mathbf{1}^{\bullet+}$, or first-order with respect to each of $\mathbf{1}^{\bullet+}$ and **1**. When the solvent/electrolyte was changed to dichloromethane/0.2 M $Bu_4N^+PF_6^-$, the reaction rate did not change significantly when compared with the rate using Me$_2$SO. CV in acetonitrile led to similar results, but the analysis of the results was complicated due to partial exchange of MeCN for coordinated Me$_2$SO (*vide infra*). We conclude that there was essentially no solvent effect on the rate of the reaction of $\mathbf{1}^{\bullet+}$ under these reaction conditions on the time scale (seconds or less) that applies to the CV measurements.

Variable-temperature DCV measurements in the temperature range 18–50 °C revealed an Arrhenius activation energy near zero (E_a = −7 ± 4 kJ mol^{-1}).[15] On the assumption that the one-electron oxidation was followed by a second-order process with respect to $\mathbf{1}^{\bullet+}$ (EC dimerization mechanism, Scheme 1),

$$Cp^*Ir(Me_2SO)Me_2 \rightleftharpoons Cp^*Ir(Me_2SO)Me_2^{\bullet+} + e^-$$

$$2\ Cp^*Ir(Me_2SO)Me_2^{\bullet+} \longrightarrow \text{Products} \qquad \text{rate} = \tfrac{1}{2}\,k[Cp^*Ir(Me_2SO)Me_2^{\bullet+}]^2$$

Scheme 1

the DCV data were converted to rate constants by comparison with theoretical working curves. The Eyring activation parameters for the bimolecular reaction of $\mathbf{1}^{\bullet+}$ were then obtained: $\Delta H^‡$ = −10 ±4 kJ mol^{-1}, $\Delta S^‡$ = −191 ± 10 J K^{-1} mol^{-1}, and k(25 °C) = 3.2 × 10^4 M^{-1} s^{-1}. Analogous variable-temperature DCV measurements were also performed for the bis(deuteriomethyl) analog **1**-d_6. Comparison of the kinetic data from these experiments resulted in a kinetic isotope effect k_H/k_D = 1.6–2.2 (the magnitude was randomly distributed over the temperature range 18–50 °C). This finding is indicative of a C–H bond cleavage in a coordinated methyl group before or during the rate-limiting step.

Chemical oxidation of Cp*Ir(Me$_2$SO)Me$_2$ in Me$_2$SO

When **1** was oxidized in Me$_2$SO using $Cp_2Fe^+BF_4^-$, the only observable Ir-containing product was again **2**(BF$_4^-$). A GC analysis of the vapor phase revealed the formation of methane and ethene in an approximate ratio of at least 20 : 1 at substrate/oxidant concentrations of 10 mM/10 mM as well as 70 mM/43 mM in Me$_2$SO, along with traces of ethane (< 0.5%). Since the oxidation potential of **1** is 0.18 V positive of the Fc couple, the Nernst equation implies a very low equilibrium concentration of $\mathbf{1}^{\bullet+}$, which could serve effectively to suppress second-order processes if they were competing with first-order ones. An effective increase in the concentration of $\mathbf{1}^{\bullet+}$ was therefore attempted by using the considerably stronger oxidant $(C_5H_5)(C_5H_4COMe)Fe^+BF_4^-$ ($E°$ = +0.25 *vs.* Fc[16]). This resulted in a much less selective process, with a mixture of largely unidentified Ir-containing products. This may indicate that the stronger oxidant is capable of intercepting and oxidizing short-lived intermediates that are not detected by CV, and that are not intercepted by Cp_2Fe^+. These results will not be elaborated further.

Isotope labeling studies

An exhaustive electrolysis was conducted using a 1 : 1 mixture of **1** and Cp*Ir(Me$_2$SO)(CD$_3$)$_2$ (**1**-d_6) followed by GC–MS analysis of the vapor phase. This revealed mainly the formation of CH_4 and CHD_3 in a *ca.* 1 : 1 ratio. Determination of the

ethene isotopomer distribution is subject to uncertainties due to the small quantity of the analyte, but is dominated by C_2H_4 (53–98%) and some C_2D_4 (1–40%).[17]

A crossover experiment using a 1 : 1 mixture of **1** and **1**-d_6, and the $Cp_2Fe^+BF_4^-$ oxidant resulted in essentially the same gaseous products as in the electrode oxidation. Thus, CH_4 and CHD_3 were produced in an approximately 1 : 1 ratio, and C_2H_4 was obtained as the major ethene isotopomer (64–91%; C_2D_4 7–34%; C_2H_3D 0–13%; $C_2H_2D_2$ 0–1%; C_2HD_3 0–4%) on the basis of a GC–MS analysis. In an attempt at tracing the origin of the hydrogen atoms in the gaseous products, oxidation of **1** was conducted in $(CD_3)_2SO$. This resulted in the exclusive formation of CH_4 and C_2H_4 by GC–MS, establishing that the fourth hydrogen atom in the methane product is not derived from the solvent. A $^2H\{^1H\}$ NMR analysis of the organometallic products demonstrated the anticipated exchange of $(CD_3)_2SO$ for coordinated $(CH_3)_2SO$ when $(CD_3)_2SO$ is used as solvent. Importantly, the analyses showed *no evidence* of deuterium incorporation into coordinated Cp* or methyl groups, contrasting with the results of the oxidation of $Cp^*Ir(PPh_3)Me_2$ in which activation of C–H bonds in the Cp* ligand occurred. We also considered the possibility that adventitious water in the Me_2SO solvent might be involved. This was probed by the oxidation of **1** with $Cp_2Fe^+BF_4^-$ in $(CD_3)_2SO$ to which was added 1% (v/v) of D_2O. The GC–MS analysis of the vapor phase in this case showed *ca.* 67% CH_4 and 33% CH_3D. A ^1H NMR analysis of the solvent/water mixture showed significant amounts of non-deuterated water; if all water had been present as D_2O, the CH_3D content would presumably have been even greater than 33%.[18] Consistently, the complementary experiment, oxidation of $Cp^*Ir[(CD_3)_2SO](CD_3)_2$ with $Cp_2Fe^+BF_4^-$ in Me_2SO to which was added 0.5% H_2O, showed predominantly the formation of CHD_3. $^2H\{^1H\}$ and ^1H NMR analysis of the organometallic products in these experiments showed, as in previous experiments, no sign of H/D scrambling into coordinated Cp* or methyl groups. This series of experiments strongly imply water—intentionally added or as a residual impurity in the Me_2SO solvent—as the origin of the fourth hydrogen atom in much, if not all of, the methane product.

Chemical and electrochemical oxidation of $Cp^*Ir(Me_2SO)Me_2$ in acetonitrile and dichloromethane

The oxidation of **1** with $Cp_2Fe^+BF_4^-$ in acetonitrile gave mostly methane, less than 30% ethane, small quantities (5%) of ethene, free Me_2SO, and a mixture of three Ir-containing compounds. The ^1H NMR spectroscopic data of the products are attributed to the compounds $Cp^*Ir(Me_2SO)_2Me^+$ (**2**), $Cp^*Ir(Me_2SO)(NCMe)Me^+$ (**3**), and $Cp^*Ir(NCMe)_2Me^+$ (**4**). Compound **2**(BF_4^-) was isolated as an air-stable, crystalline material after protonolysis of **1** with $HBF_4{\cdot}Et_2O$ in Me_2SO (see the Experimental section). The X-ray crystal structure of **2**(BAr_f^-)[7] has also been determined (*vide infra*). The cation **2** displayed ^1H NMR signals (CD_2Cl_2) at δ 3.35 and 3.36 (diastereotopic methyl groups in each S-coordinated Me_2SO), 1.83 (Cp*), and 0.96 (Ir–Me). Compounds **3** and **4** were observed *in situ*, but not isolated. The ^1H NMR spectrum of **3** (acetonitrile-d_3) displayed signals at δ 0.57 (Ir–Me), 1.75 (Cp*), 3.05 and 3.21 (diastereotopic methyls of S-coordinated Me_2SO); coordinated MeCN was not observed due to exchange with the solvent. For **4**, the ^1H NMR spectrum exhibited resonances at δ 0.68 (Ir–Me) and 1.75 (Cp*); again, coordinated MeCN was not seen due to exchange with the solvent. Coordinated MeCN was however, seen in the ^1H NMR spectrum of **3** when the oxidation was conducted in acetonitrile and $CDCl_3$ was used as NMR solvent. Compound **4** is only observed when the NMR analysis is conducted in acetonitrile-d_3, hence coordinated MeCN in **4** could not be observed (see the Experimental section for details). Upon addition of Me_2SO to the mixture in CD_3CN, the relative amounts of **3** and **4** changed and signals possibly corresponding to **2** appeared at δ 0.83 (Ir–Me) and 3.21 (coordinated Me_2SO). When the solvent was removed by evaporation (leading to a gradual increase of the Me_2SO concentration) and the residue was dissolved in CD_2Cl_2, the ^1H NMR analysis revealed **2** as the major species present. These observations suggest that **2**, **3**, **4**, Me_2SO, and MeCN are involved in a solvent-dependent equilibrium. Of the three products, we have been able to produce only **2** as a pure complex, since **3** and **4** will always exist as an equilibrium mixture. Removal of the solvent by evaporation ultimately leads to a gradual enrichment of **2** and **3** at the expense of **4** since the concentration of Me_2SO increases as acetonitrile is first removed. It is interesting to note that acetonitrile-d_3 solutions of **1** show no evidence for exchange of acetonitrile-d_3 for Me_2SO by ^1H NMR analysis.

Exhaustive electrolysis of **1** in acetonitrile/$Bu_4N^+PF_6^-$ by constant potential coulometry at $E = 0.11$–0.12 V *vs.* E°(**1**) indicated a one-electron oxidation of **1** ($n_{obs} = 0.92 \pm 0.06$ F mol^{-1}). An analysis of the organometallic products by ^1H NMR spectroscopy showed a product mixture quite similar to that obtained from the chemical oxidation. Furthermore, as previously mentioned, the DCV reaction-order analysis in acetonitrile/0.1 M $Bu_4N^+PF_6^-$ established a second-order process with respect to $\mathbf{1}^{\bullet+}$ (or $\mathbf{1}^{\bullet+}$ and **1** combined). The DCV data gave an Arrhenius activation energy close to the value measured in Me_2SO, and a decrease in the reaction rate to approximately 1/3–1/4 of the rate observed in Me_2SO ($E_a = -4 \pm 4$ and -8 ± 2 kJ mol^{-1} in two separate experiments[15]). The similarities in behavior and kinetic parameters in the two solvents Me_2SO and MeCN suggest that $\mathbf{1}^{\bullet+}$ reacts by the same, or by very similar, mechanisms in the two solvents. The complex mixture obtained in acetonitrile would then be a result of subsequent reactions. Alternatively, the complexity could arise from facile substitution of MeCN for Me_2SO in $\mathbf{1}^{\bullet+}$ (it has been firmly established[19] that very rapid ligand substitution reactions can occur by associative mechanisms at 17-electron radicals).

A ^1H NMR analysis of the $Cp_2Fe^+BF_4^-$ oxidation of **1** in dichloromethane-d_2 at temperatures below -5 °C revealed a complicated spectrum exhibiting at least three major resonances in the Cp* region (δ 1.55–1.80) in addition to those of **1**, and a singlet at δ 12.3. There were no obvious signs of paramagnetic species. Inverse ^1H–^{13}C correlated NMR spectroscopy (HSQC) analysis showed a weak interaction between the proton signal at δ 12.3 and a carbon atom resonating at δ 212 (this signal could only be seen because of the enhanced sensitivity caused by the observation of the ^1H signal), thus pointing to a possible carbenic intermediate (see discussion below). The signal at δ 12.3 was not observed when trace amounts of Me_2SO (less than 1% v/v) were added prior to the reaction.

Oxidation of $Cp^*Rh(Me_2SO)Me_2$ (6) in Me_2SO

Oxidation of the Rh compound $Cp^*Rh(Me_2SO)Me_2$ (**6**) with one equivalent of $Cp_2Fe^+BF_4^-$ led to the exclusive formation of ethane and $Cp^*Rh(Me_2SO)_2Me^+$ (**7**) as judged from GC and ^1H NMR analyses. This result appears to be in accord with the behavior of the previously investigated Rh complexes $Cp^*Rh(PPh_3)Me_2$[3f] and Cn^*RhMe_3.[3j]

In both these cases it was shown that the reductive elimination of ethane was intramolecular, presumably yielding the intermediates $Cp^*Rh(PPh_3)^{\bullet+}$ and $Cn^*RhMe^{\bullet+}$, respectively. Further oxidation and either solvent coordination or comproportionation would ultimately yield $Cp^*Rh(PPh_3)(NCMe)_2^{2+}$ and a mixture of $Cn^*Rh(NCMe)Me_2^+$ and $Cn^*Rh(NCMe)_2Me^{2+}$ respectively, which were the first observed organometallic products. In the presence of acetonitrile, $Cp^*Rh(PPh_3)Me_2$ and $Cp^*Rh(PPh_3)(NCMe)_2^{2+}$ were shown to undergo comproportionation to give $Cp^*Rh(PPh_3)(NCMe)Me^+$, and therefore the ultimate product resembles the formation of **7** from oxidation of **6** in Me_2SO. The comproportionation of the phosphine

analogs is, however, much slower (time scale several hours) than the reductive elimination [k(20 °C) = 96 s^{-1} in acetonitrile], contrasting a possibly direct formation of **7** from $\mathbf{6}^{\bullet+}$.

The Rh complex **6** exhibited a chemically irreversible cyclic voltammogram (E_p = 0.22 V *vs.* Fc) at v = 1.0 V s^{-1}. The irreversibility persisted even at v = 50 V s^{-1}, thus the follow-up chemical reaction of electrode-generated $\mathbf{6}^{\bullet+}$ was too fast for a detailed voltammetric investigation of the kinetics and reaction mechanism using our experimental setup. However, the qualitative findings are indicative of some fundamental differences in the reactivities of analogous Rh and Ir complexes, as will be elaborated later.

X-Ray crystal structure determinations

More convenient syntheses of Cp*Ir(Me_2SO)Me_2 (**1**) and Cp*-Rh(Me_2SO)Me_2 (**6**), using dimethylzinc in place of trimethyl aluminium reagents, were developed (see the Experimental section). The two compounds are isomorphous, have a pseudo-octahedral ligand arrangement about the metal center and, as Rh(III) and Ir(III) are virtually the same size,[20] show only minor differences in bond lengths and angles. Fig. 2 (top) shows a

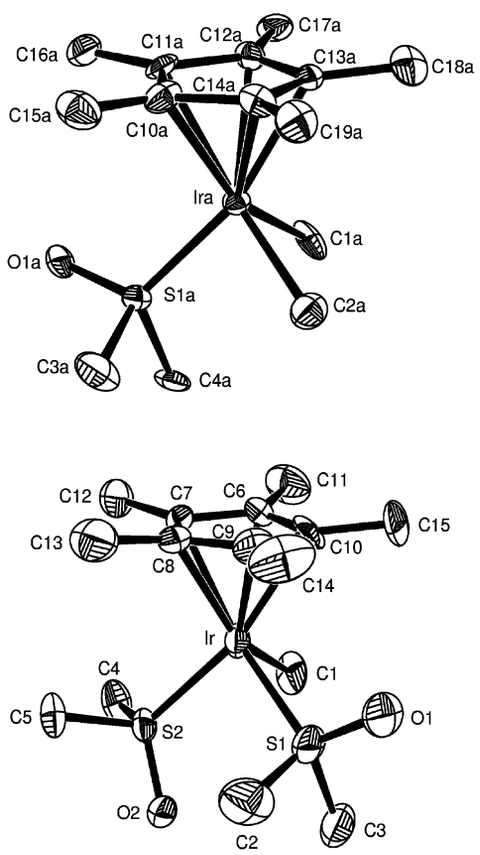

Fig. 2 ORTEP[27] structures of Cp*Ir(Me_2SO)Me_2 (**1**, top) and Cp*-Ir(Me_2SO)$_2Me^+$ (**2**, bottom). Hydrogen atoms have been omitted for clarity.

perspective view of Cp*Ir(Me_2SO)Me_2 (the Rh analog is not shown because of the close structural resemblance to **1**, *vide infra*). Key bond lengths and angles for **1** and **6** are given in Tables 1 and 2, respectively and details of data collection and refinement are summarised in Table 4 in the Experimental section.

The salt Cp*Ir(Me_2SO)$_2Me^+BAr_f^-$ **2**(BAr_f^-) was obtained by protonolysis of **1** with $HBF_4 \cdot Et_2O$ followed by anion exchange with $Na^+BAr_f^-$ in dichloromethane (see the Experimental section). The X-ray structure (150 K) of this species was also determined. Fig. 2 (bottom) includes an ORTEP plot of the

Table 1 Selected interatomic distances (Å) and angles (°) in Cp*Ir(Me_2SO)Me_2 (**1**)

	Molecule A	Molecule B
Ir–S(1)	2.203(2)	2.206(2)
Ir–C(1)	2.11(1)	2.10(1)
Ir–C(2)	2.15(1)	2.13(1)
S(1)–O(1)	1.495(7)	1.477(7)
Ir–Cp* centroid	1.886 ave.	
S(1)–Ir–C(1)	91.4(3)	92.7(3)
S(1)–Ir–C(2)	90.0(3)	89.9(3)
C(1)–Ir–C(2)	83.3(5)	83.2(5)
Ir–S(1)–O(1)	118.0(3)	118.1(3)

Table 2 Selected interatomic distances (Å) and angles (°) in Cp*Rh(Me_2SO)Me_2 (**6**)

	Molecule A	Molecule B
Rh–S(1)	2.211(1)	2.210(1)
Rh–C(1)	2.090(4)	2.099(5)
Rh–C(2)	2.092(4)	2.103(5)
S(1)–O(1)	1.484(3)	1.480(3)
Rh–Cp* centroid	1.889 ave.	
S(1)–Rh–C(1)	92.0(1)	92.2(1)
S(1)–Rh–C(2)	90.9(1)	91.2(2)
C(1)–Rh–C(2)	83.2(2)	82.9(2)
Rh–S(1)–O(1)	117.7(1)	117.6(1)

Table 3 Selected distances (Å) and angles (°) in the cation part of **2**(BAr_f^-)

Ir–S(1)	2.283(2)	S(1)–Ir–S(2)	93.21(8)
Ir–S(2)	2.263(2)	S(1)–Ir–C(1)	87.5(3)
Ir–C(1)	2.119(8)	S(2)–Ir–C(1)	85.3(3)
Ir–Cp* centroid	1.886		

cationic part of **2**(BAr_f^-). The anion was unexceptional and is included in the ESI.† Table 3 shows selected bond distances and angles in the cation, and crystal structure data are included in Table 4.

In each of the three structures analyzed, the complex adopts the geometry of a three-legged pianostool, with Cp* as the base and the methyl and S-coordinated Me_2SO ligands as the legs. The Cp*(centroid)–M distances are 1.886 Å and 1.889 Å for **1** and **6** respectively (these are averages as there are two independent molecules per asymmetric unit). The Me_2SO ligand is S-bound with metal–S bond lengths of 2.205(2) and 2.211(1) Å for M = Ir and Rh, respectively. The Ir–S distances in **2** are slightly different [2.263(2) and 2.283(2) Å] and slightly longer than those in **1** and **6**, possibly for steric reasons. The metal–methyl carbon bond lengths (average values for crystallographically independent molecules) of 2.122 (**1**), 2.096 (**6**), and 2.119(8) Å for (**2**) are normal. The Ir–Me and Ir–Cp*(centroid) bond distances of **2** are close to those of **1** [**1**: Ir–Me 2.11(1) and 2.14(1) Å, Ir–Cp* 1.886 Å]. The S–Ir–S and S–metal–Me bond angles reflect the pseudo-octahedral coordination geometry around the metal center and the greater steric demands of the Me_2SO compared to the methyl group. Thus, the angles (degrees) at the metal increase in the order Me–Ir–Me 83.3 (av. in **1**) ≈ Me–Rh–Me 83.0 (av. in **6**) < Me–Ir–S 85.3 and 87.5 (in **2**) < Me–Ir–S 90.0 and 92.0 (av. in **1**) ≈ Me–Rh–S 91.0 and 92.1 (av. in **6**) < S–Ir–S 93.2° (in **2**). The chief feature is that the angles reflect the greater steric demands of the S-bonded Me_2SO by comparison with Me, thus, S–metal–S > S–metal–C > C–metal–C. It also appears that in the cation **2**, the S–metal–C angle is somewhat larger than in the neutral complexes **1** and **6**. The Me_2SO ligand with the shortest bond to the metal center also exhibits the smallest S–Ir–Me angle.

Table 4 X-Ray crystallographic data for **1**, **6**, and **2**(BAr_f^-)

Compound	**1**	**6**	**2**(BAr_f^-)
Chemical formula	$C_{14}H_{27}OIrS$	$C_{14}H_{27}ORhS$	$C_{47}H_{42}BF_{24}IrO_2S_2$
FW	435.62	346.33	1361.97
Crystal system	Triclinic	Triclinic	Monoclinic
Space group	$P\bar{1}$ (no. 2)	$P\bar{1}$ (no. 2)	$P2_1/n$
Z	4	4	4
a/Å	8.832(1)	8.813(1)	13.547(1)
b/Å	12.913(2)	12.864(1)	25.816(4)
c/Å	14.394(2)	14.435(2)	16.645(3)
α/°	99.865(2)	100.266(2)	90
β/°	96.010(2)	96.114(2)	112.06(1)
γ/°	93.146(2)	93.100(2)	90
Volume/Å^3	1604.0(3)	1596.6(3)	5395(1)
ρ_{calc}/g cm^{-3}	1.804	1.441	1.677
Crystal dimensions/mm	0.23 × 0.16 × 0.08	0.25 × 0.15 × 0.09	0.2 × 0.3 × 0.4
Temperature/K	150	150	150
Diffractometer	Bruker P4/RA/-SMART 1000 CCD	Bruker P4/RA/-SMART 1000 CCD	Siemens SMART CCD
Radiation	MoKα	MoKα	MoKα
2θ limit/°	56.6	56.6	57.5
No. of data collected	8389	8389	28879
No. of unique data	7262	7226	11609
No. of observed data ($I > 2\sigma(I)$)	5991	5407	8490
Agreement between equivalent data (R_{int})	0.081	0.047	0.062
No. of parameters varied	322	322	714
μ/mm^{-1}	8.440	1.186	2.67
Absorption correction	Gaussian integration (face-indexed)	Gaussian integration (face-indexed)	Analytical (xprep, Siemens 1997)
R_1 (F_0)	0.0576	0.0394	0.0655
wR_2 (F_0^2) ($I > 2\sigma$)	0.1593	0.0928	0.1344

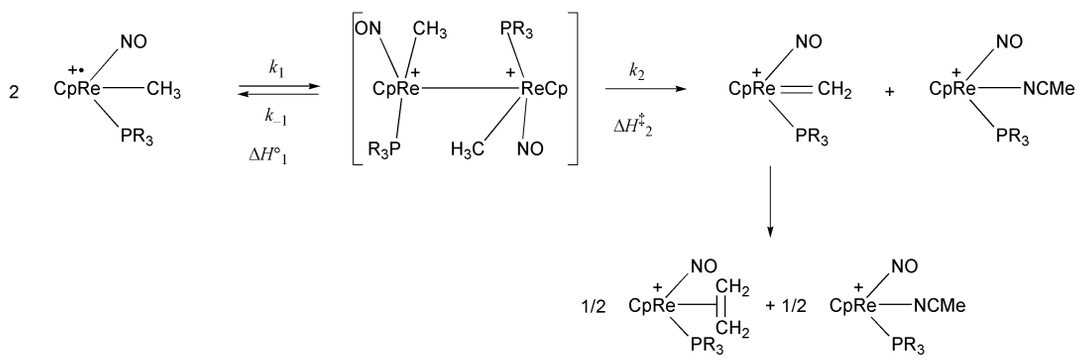

Scheme 2

Discussion

Mechanistic aspects of the oxidation of Cp*Ir(Me$_2$SO)Me$_2$

The ratio of methane to ethene formed from the chemical and electrochemical one-electron oxidations of **1** showed some differences depending on the reaction conditions. However, the similarities suggest that the fundamental chemistry that is initiated by the one-electron process is similar in both cases. The electrochemical results, in particular the quantitative DCV data, shed some light on features of the oxidation mechanism under the particular reaction conditions and on the relatively short (less than a second) CV timescale. The following features are particularly interesting: (1) the reaction of $\mathbf{1}^{\bullet+}$ is *second order in Ir*, (2) the enthalpy of activation is near zero and the entropy of activation is strongly negative, the latter being consistent with the second-order nature of the reaction, and (3) there is an appreciable k_H/k_D kinetic isotope effect for the reaction of Ir–CH_3 *vs.* Ir–CD_3.

The formation of ethene together with the reactivity implied by the quantitative DCV data is reminiscent of the behavior that was observed for the oxidation of CpRe(NO)(PR$_3$)Me (R = Ph,[21] Me[14a]), interpreted according to Scheme 2. The reactions of the Re cation radicals were also second-order processes with low (even negative) values for $\Delta H^{\ddagger}$, strongly negative $\Delta S^{\ddagger}$, and kinetic isotope effects k_H/k_D in the range 2–3. The first observed products in acetonitrile were 1 : 1 : 1 molar ratios of CpRe(NO)(PR$_3$)(=CH$_2$)$^+$, CH_4, and CpRe(NO)(PR$_3$)(NCMe)$^+$. The methylene complex underwent quantitative intermolecular ligand coupling in a slower step to give equimolar amounts of the ethene complex CpRe(NO)(PR$_3$)(CH$_2$=CH$_2$)$^+$ and CpRe(NO)(PR$_3$)(NCMe)$^+$. The low values observed there for $\Delta H^{\ddagger}$ result from the negative ΔH°_1 for the exothermic preequilibrium dimerization canceling, in part, the positive $\Delta H^{\ddagger}_2$ for the rate-limiting step.

In the present case, however, the amounts of ethene formed are far less than would be expected from a mechanism analogous to that outlined in Scheme 2. A possible reason may be that two mechanisms operate in parallel, one forming methane and the other giving ethene (or both) (Scheme 3). One might expect at least one additional organometallic product to be formed in such a case (although the diverging pathways might conceivably converge on the same organometallic product). Taking into account that the chemical oxidation generates only 5–6% of ethene, the amounts of the putative alternative organometallic product(s) may well be close to the detection limit of the ^{1}H NMR analysis and these species may remain unobserved. In the case of electrochemical oxidation, somewhat larger amounts of ethene are produced (12–13%). However, in this case the NMR analysis of the product mixtures are preceded by dichloromethane extraction and

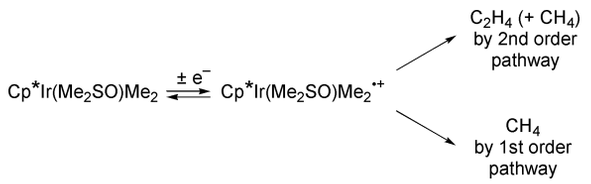

Scheme 3

work-up (see the Experimental section for details), and it is conceivable that the products from the proposed second-order ethene forming reaction path in Scheme 3 may be lost during work-up.

It is well known that Cp*Ir complexes readily form dinuclear species, for example μ-hydride and μ-methylene complexes.[22] Furthermore, the dimerization of the $Cp^*Ir(CO)_2$ moiety gives a variety of di-iridium species[23] including $[\{Cp^*Ir(CO)_2\}_2]^{2+}$. It is important to appreciate that the CV experiments, carried out on a stationary solution, measure what happens to $\mathbf{1}^{\bullet+}$ under conditions where the local concentration of $\mathbf{1}^{\bullet+}$ is rather high in the undisturbed diffusion layer at the electrode surface. On the other hand, the bulk electrolysis is performed on a vigorously stirred solution of **1** with an experimental timescale of a few minutes. Under these conditions, $\mathbf{1}^{\bullet+}$ is effectively transported away from the electrode diffusion layer and diluted into the bulk solution before significant reaction can occur. Consequently, second-order reactions of $\mathbf{1}^{\bullet+}$, which should give equal amounts of methane and ethene on a carbon basis, will be less favored and may be suppressed by competing first-order pathways, giving only methane, that are not kinetically significant and therefore not detected in the CV experiments. Chemical oxidation with $Cp_2Fe^+BF_4^-$ occurs under conditions where the equilibrium concentration of $\mathbf{1}^{\bullet+}$ is relatively low; the second-order reaction that is implied by the CV data is again attenuated due to significant contributions from the competing first-order pathway.

The most obvious reaction that would produce **2** from **1** with deuterium incorporation from added water would be a protonolysis of **1**. However, solutions of **1** in Me_2SO-d_6 are stable on the timescale of the oxidation reactions, rendering this explanation unattractive. Other possibilities include a protonolysis of 17-electron $\mathbf{1}^{\bullet+}$ or—perhaps more likely—of an electron-rich, 19-electron Me_2SO adduct $Cp^*Ir(Me_2SO)_2Me_2^{\bullet+}$. The oxidizing reaction conditions may generate a more acidic medium than would have been the case without the oxidant.

Comparison of reactivities of $Cp^*M(Me_2SO)Me_2$ and $Cp^*M(PPh_3)Me_2$ for M = Rh, Ir

Due to the stronger donor power of PPh_3 compared to Me_2SO, the oxidation potentials of $Cp^*Rh(PPh_3)Me_2$ (0.04 V *vs.* Fc in MeCN–CH_2Cl_2 9 : 1)[3f] and $Cp^*Ir(PPh_3)Me_2$ (−0.01 V in MeCN)[3g] are markedly lower than those of the corresponding $Cp^*M(Me_2SO)Me_2$ compounds **1** (0.18 V in MeCN) and **6** (E_p = 0.22 V in MeCN; this represents a *minimum* value due to the unknown kinetic potential shift caused by the rapid homogeneous reaction of $\mathbf{6}^{\bullet+}$). This may also, in part, help explain the significant differences in the rates of the oxidatively induced reactions of the PPh_3 *vs.* Me_2SO pairs: whereas the rate constant for the oxidatively induced reaction of $Cp^*Rh(PPh_3)Me_2$ is close to 100 s^{-1} at 20 °C, **6** reacts too fast (> 1000 s^{-1}) to be measured in our labs. The pair **1** and $Cp^*Ir(PPh_3)Me_2$ exhibit a similar trend, as the Me_2SO compound displays a considerably higher reaction rate [k(25 °C) = 3.2 × 10^4 M^{-1} s^{-1}] than the PPh_3 analog, which reacts too slowly to be measured by cyclic voltammetry. The enhanced electron deficiency of **1** and **6** compared to the PPh_3 complexes might be expected to provide kinetically more reactive radical cations, which in all cases undergo reactions that are, at least formally, reductive elimination reactions as defined in a broad sense in eqns. (1)–(3). The reduced steric bulk of the Me_2SO *vs.* the PPh_3 ligand may also be a contributing factor.

Concluding remarks

The differences in reactivities of $Cp^*Ir(Me_2SO)Me_2$ and its Rh analog upon oxidation are striking. As elaborated in the Introduction, marked differences exist for other systems of these metals as well. It is a generally accepted trend that metal–carbon, metal–hydrogen, and metal–metal bond dissociation energies increase on descending from second- to third-row metals in the Periodic table. The Rh di- and tri-alkyl compounds $Cp^*Rh(PPh_3)Me_2$ and Cn^*RhMe_3 both yield carbon–carbon coupling products upon oxidation, involving simultaneous *bond breaking* of two metal–carbon bonds in the same molecule. The mechanism for the oxidation of $Cp^*Rh(Me_2SO)Me_2$ is not known but the fact that ethane is formed as the only organic product suggests that the same applies here. In contrast, the Ir dialkyls $Cp^*Ir(PPh_3)Me_2$ and $Cp^*Ir(Me_2SO)Me_2$ appear to react after oxidation by mechanisms that involve *bond formation* as a key step (Ir insertion into a Cp* C–H bond for L = PPh_3; Ir–Ir bond formation, possibly *via* an Ir–Me–Ir bridge, for L = Me_2SO under conditions that favor second-order reactivity). The organic products are eliminated in a subsequent step. These divergent reaction paths are fully consistent with the relative strengths of bonds to second- *vs.* third-row metals. Analogous differences may be anticipated for other pairs of metals as well, and will have important implications for the use of second- *vs.* third-row metals in catalysis.

Experimental

General procedures

All operations were carried out under an atmosphere of Ar (for electrochemical experiments) or N_2 with the use of vacuum line, Schlenk, syringe, or drybox techniques. THF and ether were distilled from blue/purple solutions of sodium benzophenone ketyl. Acetonitrile, Me_2SO, and dichloromethane were distilled from CaH_2. Me_2SO was further stored over activated 4 Å molecular sieves. ^1H NMR and $^{13}C\{^1H\}$ NMR spectra were recorded on Bruker Avance DXP 300, Bruker ACS 250, and Bruker AMX 400 instruments. All NMR spectra are reported in ppm (δ) relative to tetramethylsilane, with the residual solvent proton resonance and carbon resonance as internal standards. IR spectra were obtained on a Nicolet 560 E.S.P FTIR spectrometer. GC analyses were conducted on Hewlett-Packard 5710A and HP 6890+ gas chromatographs using a 30 m × 0.54 mm Megabore GS-Q capillary column. The elemental analyses were carried out at the elemental analysis laboratory, Department of Chemistry, University of Sheffield. The GC–MS analyses were carried out with a Fisons GC 8000 gas chromatograph (5 m × 0.25 mm Chrompack CP-SIL fused silica column) interfaced to a Fisons VG ProSpec-Q mass spectrometer, and with a Fisons 8060 gas chromatograph (30 m × 0.22 mm SGE BPX5 fused silica column) interfaced to a Micromass ProSpec magnetic sector mass spectrometer.

Electrochemical measurements were performed on an EG&G-PAR Model 273 potentiostat/galvanostat driven by an external HP 3314A function generator. The signals were fed to a Nicolet 310 digital oscilloscope and processed by an online personal computer. The working electrodes were Pt disk electrodes (d = 0.4–1.0 mm). The counter electrode was a Pt wire, and the Ag wire reference electrode assembly was filled with acetonitrile/0.01 M $AgNO_3$/0.1 M $Bu_4N^+PF_6^-$. The reference electrode was calibrated against the Cp_2Fe/Cp_2Fe^+ (Fc) couple. The positive feedback *iR* compensation circuitry of the potentiostat was employed. A Pt gauze working electrode was used for the constant potential coulometry and preparative

electrolysis experiments. The electrochemical experiments in Me_2SO and acetonitrile were carried out at 20–25 °C unless otherwise stated, and at 0 °C in dichloromethane.

Syntheses

$Cp_2Fe^+BF_4^-$ and $Cp(C_5H_4COMe)Fe^+BF_4^-$ were prepared from the appropriately substituted ferrocenes with $AgBF_4$,[16] and $(CD_3)_2Mg$,[24] $[Cp^*IrCl_2]_2$,[25] and $Na^+BAr_f^-$ [26] were prepared according to published procedures.

$Cp^*Ir(Me_2SO)Me_2$. A more convenient synthesis than the published one using Al_2Me_6 [9a] was as follows: $ZnMe_2$ (130 μL of a 2.0 M solution in toluene, Aldrich; 0.260 mmol) was added to $Cp^*IrBr_2(Me_2SO)$ (102 mg, 0.18 mmol) in THF (10 mL) at −80 °C. The solution was warmed to room temperature and stirred (30 min) and was then hydrolyzed by adding water (100 μL). The solvent was removed *in vacuo* and the residue extracted in air with CH_2Cl_2 (3 × 5 mL). The extracts were filtered through Celite and the solvent was removed under reduced pressure. The residue was then extracted with *n*-pentane (5 × 5 mL doped with Me_2SO) and filtered, and the solvent volume was reduced to *ca.* 5 mL. The solution was cooled at −20 °C for 16 h to give the product as pale yellow crystals (51 mg, 64%).

$Cp^*Rh(Me_2SO)Me_2$. Was obtained as large yellow crystals (1.9 g, 85%) by a similar reaction sequence, starting from $[Cp^*RhCl_2]_2$ (2.0 g, 3.2 mmol) and $ZnMe_2$ (5 mL of a 2.0 M solution). Both compounds were spectroscopically identical to authentic samples and their identities were further confirmed by an X-ray crystal structure determination of each.

$Cp^*Ir(Me_2SO)(CD_3)_2$ (1-d_6). $[Cp^*IrCl_2]_2$ (50 mg, 0.063 mmol) was dissolved in THF (10 mL) and Me_2SO (30 μL, 0.42 mmol) was added while stirring. The solution was cooled to −78 °C and a 0.05 M solution of $(CD_3)_2Mg$ in THF (2 mL, 0.1 mmol) was added dropwise. The mixture was slowly warmed to room temperature, and stirring was continued for 2 days after which wet THF (THF–water 3 : 1) was added dropwise to ensure that no $(CD_3)_2Mg$ was left as evidenced by the cessation of gas evolution. The volatiles were removed *in vacuo*, and the product was extracted with pentane (10 mL). The extract was filtered and washed with water (2 × 5 mL) to remove most of the monomethylated contaminant. The solution was dried over $MgSO_4$ for 30 min and filtered. The solvent was removed under vacuum, and the product was purified by sublimation at 40 °C/1.5 mm Hg to give a yellow solid (11 mg, 20%). Use of excess $(CD_3)_2Mg$ should be avoided since this leads to the formation of $Cp^*Ir(CD_3)_4$ which is difficult to separate from the desired product (separation is possible by flash chromatography using silica–toluene, but this leads to lower yields). The isotopic purity of **1**-d_6 was checked by ^1H NMR spectroscopy, and we estimate the complex to be more than 99% deuterated at the Ir-methyl groups. ^1H NMR ($CDCl_3$, 300 MHz) δ 1.69 (s, 15 H, C_5Me_5), 2.89 (s, 6 H, Me_2SO).

$Cp^*Ir(Me_2SO)_2Me^+BF_4^-$ [2(BF_4^-)]. $HBF_4{\cdot}Et_2O$ (33 μL, 0.22 mmol) was added dropwise to a stirred solution of $Cp^*Ir(Me_2SO)Me_2$ (100 mg, 0.23 mmol) and Me_2SO (160 μL, 2.25 mmol) in ether (5 mL), leading to the instantaneous precipitation of a yellow-white solid. The volatiles were removed *in vacuo* and the residue was washed with ether (6 × 2 mL). The residue was dissolved in dichloromethane, the solution was filtered through Celite, and the solvent was removed *in vacuo* yielding the product as a pale yellow solid (131 mg, 99%). ^1H NMR (CD_2Cl_2, 300 MHz) δ 0.96 (s, 3 H, Ir*Me*), 1.83 (s, 15 H, C_5Me_5), 3.35 (s, 6 H, Me_2SO), 3.36 (s, 6 H, Me_2SO). $^{13}C\{^1H\}$ NMR ($CDCl_3$, 62.9 MHz) δ −16.0 (Ir*Me*), 8.6 (C_5Me_5), 45.5, 47.2 (Me_2SO), 100.4 (C_5Me_5). Anal. calc. for $C_{15}H_{30}BF_4IrO_2S_2$: C, 30.76; H, 5.17; S, 10.95. Found: C, 30.45; H, 5.06; S, 10.96%.

$Cp^*Ir(Me_2SO)_2Me^+BAr_f^-$ [2(BAr_f^-)]. To a solution of **2**(BF_4^-) (30 mg, 51 μmol) in dichloromethane (10 mL) was added $Na^+BAr_f^-$ (45 mg, 51 μmol) and the mixture was stirred at ambient temperature for 1 h. The volatiles were removed *in vacuo* and the product was extracted from the mixture by dissolving in toluene. Filtration through Celite and evaporation of the solvent gave the product in quantitative yield. X-Ray quality crystals were obtained by slow evaporation of diethyl ether into a solution of **2**(BAr_f^-) in CH_2Cl_2. ^1H NMR ($CDCl_3$, 200 MHz) δ 0.92 (s, 3 H, Ir*Me*), 1.66 (s, 15 H, C_5Me_5), 3.17 (s, 12 H, 2 Me_2SO), 7.52 (s, 4 H, *p*-H at BAr_f^-), 7.69 (br, 8 H, *o*-H at BAr_f^-).

Constant-potential coulometry experiments

The experiments were conducted using 3–4 mM solutions of the substrate in an electrolyte solution of 0.05–0.06 M $Me_4N^+BF_4^-$ in Me_2SO unless otherwise described. The electrode potential was maintained at +0.1 V relative to $E°_{ox}$(**1**). An H-shaped electrolysis cell was used, in which the two cell compartments were separated by a grade 4 glass frit junction. Each compartment was filled with 15–20 mL of electrolyte solution. For gas analysis experiments, a modified electrolysis cell was used. This cell was equipped with a gas-tight reaction compartment with a rubber septum for withdrawal of gas samples.

Chemical oxidation of $Cp^*M(Me_2SO)Me_2$ (M = Ir, Rh) with $Cp_2Fe^+PF_6^-$—analysis of the organometallic and gaseous products

A 5 mL Schlenk flask was loaded with a magnetic stirrer and the solid reagents (typically *ca.* 10 mg of the substrate, 23 μmol for M = Ir). A slight excess of the substrate was used to ensure complete consumption of the oxidant, thereby avoiding the presence of paramagnetic species in the product mixture. The flask was fitted with a septum and the solvent (5 mL) was added by syringe while stirring. For the Ir complex, the complete consumption of the oxidant took place during a 2–4 h period as judged by the complete color change from blue, *via* green, to yellow-orange, whereas oxidation of the Rh complex was complete in a few seconds. Gas samples for GC or GC–MS measurements were withdrawn by syringe from the headspace above the solution. The volatiles were removed *in vacuo* and the residue was subjected to analysis by ^1H NMR spectroscopy.

Chemical oxidation of $Cp^*Ir(Me_2SO)Me_2$ in acetonitrile. A 5 mL round-bottomed flask was loaded with $Cp^*Ir(Me_2SO)Me_2$ (6.9 mg, 0.016 mmol) and $Cp_2Fe^+BF_4^-$ (4.2 mg, 0.015 mmol). Acetonitrile (2 mL) was added while stirring, and stirring was continued for 30 min. The volatiles were removed *in vacuo* and the residue was dissolved in $CDCl_3$. ^1H NMR ($CDCl_3$, 300 MHz) **2**: δ 0.92 (s, 3 H, Ir*Me*), 1.82 (s, 15 H, C_5Me_5), 3.38 (s, 2 × 6 H, Me_2SO); **3**: δ 0.74 (s, 3 H, Ir*Me*), 1.75 (s, 15 H, C_5Me_5), 2.56 (s, 3 H, *Me*CN), 3.09 (s, 3 H, Me_2SO), 3.48 (s, 3 H, Me_2SO). Electrospray MS (MeCN reaction mixture): *m*/*z* calc. for $[C_{15}H_{24}IrN_2]^+$ (M^+ of **4**) 423, 424, 425, 426, 427; found *m*/*z* = 423, 424, 425, 426, 427; also *m*/*z* = 382, 383, 384, 385, 386 [M^+ − MeCN].

Chemical oxidation of $Cp^*Ir(Me_2SO)Me_2$ in acetonitrile-d_3. An NMR tube fitted with a ground-glass joint was loaded with $Cp^*Ir(Me_2SO)Me_2$ (7.7 mg, 0.018 mmol) and $Cp_2Fe^+BF_4^-$ (3.9 mg, 0.014 mmol). The solvent (0.5 mL) was added by vacuum transfer and the tube was flame sealed under vacuum. ^1H NMR (CD_3CN, 200 MHz) **2**: not observed; **3**: δ 0.57 (s, 3 H, Ir*Me*), 1.75 (s, 15 H, C_5Me_5), 3.05 (s, 6 H, Me_2SO), 3.21 (s, 6 H, Me_2SO); **4**: δ 0.68 (s, 3 H, Ir*Me*), 1.75 (s, 15 H, C_5Me_5). The tube was opened and equipped with a rubber septum. $(CH_3)_2SO$ (5–10 μL) was added by syringe and a ^1H NMR analysis was conducted. The solvent was then removed *in vacuo*, CD_2Cl_2 added, and another ^1H NMR analysis was performed. The findings are included in full in the Results section.

$Cp^*Rh(Me_2SO)_2Me^+$ spectroscopic data

^1H NMR (CD_2Cl_2, 200 MHz) δ 0.96 (d, $J = 2.3$ Hz, 3 H, Rh*Me*), 1.77 (s, 15 H, C_5Me_5), 3.15 (s, 6 H, Me_2SO), 3.20 (s, 6 H, Me_2SO).

X-Ray crystal structure determinations

X-Ray diffraction quality crystals of **1** and **6** were obtained by slow cooling of concentrated *n*-pentane solutions of the compounds to −20 °C. $Cp^*Ir(Me_2SO)Me_2$ and $Cp^*Rh(Me_2SO)Me_2$ crystallized in the $P\bar{1}$ (no. 2) space group. Details of data collection and refinement are summarised in Table 4.

CCDC reference numbers 169020–169022.

See http://www.rsc.org/suppdata/dt/b1/b107451m/ for crystallographic data in CIF or other electronic format.

Acknowledgements

We thank Harry Adams (University of Sheffield) and Dr Robert MacDonald (University of Alberta, Edmonton) for collecting the X-ray data for **1** and **6** and solving their structures, Simon Thorpe for kind assistance with labeling studies, Dr Tony Haynes for helpful discussions, the EPSRC for support (grant no. GR/L94192Z/01), and the British Council/Research Council of Norway Collaborative Scheme for travel grants.

References and notes

1 (*a*) J. P. Collman, L. S. Hegedus, J. R. Norton and R. G. Finke, *Principles and Applications of Organotransition Metal Chemistry*, University Science Books, Mill Valley, 1989.

2 (*a*) J. Y. Chen and J. K. Kochi, *J. Am. Chem. Soc.*, 1977, **99**, 1450; (*b*) W. H. Tamblyn, R. J. Klingler, W. S. Hwang and J. K. Kochi, *J. Am. Chem. Soc.*, 1981, **103**, 3161; (*c*) R. J. Klingler, J. C. Huffman and J. K. Kochi, *J. Am. Chem. Soc.*, 1982, **104**, 2147; (*d*) J. C. Kotz, W. Vining, W. Coco, R. Rosen, A. R. Dias and M. H. Garcia, *Organometallics*, 1983, **2**, 68; (*e*) R. F. Jordan, R. E. LaPointe, C. S. Bajgur, S. F. Echols and R. Willett, *J. Am. Chem. Soc.*, 1987, **109**, 4111; (*f*) T. Aase, M. Tilset and V. D. Parker, *J. Am. Chem. Soc.*, 1990, **112**, 4974; (*g*) M. R. Burk, W. Tumas, M. D. Ward and D. R. Wheeler, *J. Am. Chem. Soc.*, 1990, **112**, 6133; (*h*) A. L. Seligson and W. C. Trogler, *J. Am. Chem. Soc.*, 1992, **114**, 7085; (*i*) S. L. Borowsky, N. C. Baenziger and R. F. Jordan, *Organometallics*, 1993, **12**, 486; (*j*) D. Zhu, S. V. Lindeman and J. K. Kochi, *Organometallics*, 1999, **18**, 2241.

3 (*a*) D. G. Morrell and J. K. Kochi, *J. Am. Chem. Soc.*, 1975, **97**, 7262; (*b*) T. T. Tsou and J. K. Kochi, *J. Am. Chem. Soc.*, 1978, **100**, 1634; (*c*) M. Almemark and B. Åkermark, *J. Chem. Soc., Chem. Commun.*, 1978, 66; (*d*) W. Lau, J. C. Huffman and J. K. Kochi, *Organometallics*, 1982, **1**, 155; (*e*) K. Ishikawa, S. Fukusumi and T. Tanaka, *Inorg. Chem.*, 1989, **28**, 1661; (*f*) A. Pedersen and M. Tilset, *Organometallics*, 1993, **12**, 56; (*g*) A. Pedersen and M. Tilset, *Organometallics*, 1994, **13**, 4887; (*h*) A. Pedersen, M. Tilset, K. Folting and K. G. Caulton, *Organometallics*, 1995, **14**, 875; (*i*) K. Koo and G. L. Hillhouse, *Organometallics*, 1995, **14**, 4421; (*j*) E. Fooladi and M. Tilset, *Inorg. Chem.*, 1997, **36**, 6021; (*k*) R. Han and G. L. Hillhouse, *J. Am. Chem. Soc.*, 1997, **119**, 8135; (*l*) M. Scmittel, A. Burghart, H. Werner, M. Laubender and R. Söllner, *J. Org. Chem.*, 1999, **64**, 3077.

4 It is frequently difficult to distinguish truly concerted reactions from two-step ones for the two-ligand eliminations in eqn. (2). See discussion in ref. 5g.

5 (*a*) O. B. Ryan, M. Tilset and V. D. Parker, *J. Am. Chem. Soc.*, 1990, **112**, 2618; (*b*) O. B. Ryan, M. Tilset and V. D. Parker, *Organometallics*, 1991, **10**, 298; (*c*) O. B. Ryan and M. Tilset, *J. Am. Chem. Soc.*, 1991, **113**, 9554; (*d*) O. B. Ryan, K.-T. Smith and M. Tilset, *J. Organomet. Chem.*, 1991, **421**, 315; (*e*) K.-T. Smith, C. Rømming and M. Tilset, *J. Am. Chem. Soc.*, 1993, **115**, 8681; (*f*) A. A. Zlota, M. Tilset and K. G. Caulton, *Inorg. Chem.*, 1993, **32**, 3816; (*g*) K.-T. Smith, M. Tilset, R. Kuhlman and K. G. Caulton, *J. Am. Chem. Soc.*, 1995, **117**, 9473; (*h*) R. J. Klingler, J. C. Huffman and J. K. Kochi, *J. Am. Chem. Soc.*, 1980, **102**, 208; (*i*) D. E. Westerberg, L. F. Rhodes, J. Edwin, W. E. Geiger and K. G. Caulton, *Inorg. Chem.*, 1991, **30**, 1107; (*j*) M. T. Costello and R. A. Walton, *Inorg. Chem.*, 1988, **27**, 2563.

6 (*a*) M. Tilset, *J. Am. Chem. Soc.*, 1992, **114**, 2740; (*b*) V. Skagestad and M. Tilset, *J. Am. Chem. Soc.*, 1993, **115**, 5077; (*c*) M. Tilset, J.-R. Hamon and P. Hamon, *Chem. Commun.*, 1998, 765; (*d*) M. Tilset, I. Fjeldahl, J.-R. Hamon, P. Hamon, L. Toupet, J.-Y. Saillard, K. Costuas and A. Haynes, *J. Am. Chem. Soc.*, 2001, **123**, 9984.

7 Abbreviations: Cp* = η^5-C_5H_5; Cn* = 1,4,7-trimethyl-1,4,7-triazacyclononane; $BAr_f^- = B[3,5\text{-}C_6H_3(CF_3)_2]_4^-$.

8 (*a*) P. Diversi, S. Iacoponi, G. Ingrosso, F. Laschi, A. Lucherini and P. Zanello, *J. Chem. Soc., Dalton Trans.*, 1993, 351; (*b*) P. Diversi, S. Iacoponi, G. Ingrosso, F. Laschi, A. Lucherini, C. Pinzino, G. Uccellobarretta and P. Zanello, *Organometallics*, 1995, **14**, 3275; (*c*) P. Diversi, V. Ermini, G. Ingrosso, A. Lucherini, C. Pinzino and F. Simoncini, *J. Organomet. Chem.*, 1998, **555**, 135; (*d*) P. Diversi, F. F. deBiani, G. Ingrosso, F. Laschi, A. Lucherini, C. Pinzino and P. Zanello, *J. Organomet. Chem.*, 1999, **584**, 73.

9 (*a*) A. Vazquez de Miguel, M. Gomez, K. Isobe, B. F. Taylor, B. E. Mann and P. M. Maitlis, *Organometallics*, 1983, **2**, 1724; (*b*) J. M. Kisenyi, G. J. Sunley, J. A. Cabeza, A. J. Smith, H. Adams, N. J. Salt and P. M. Maitlis, *J. Chem. Soc., Dalton Trans.*, 1987, 2459; (*c*) M. Gomez, P. I. W. Yarrow, D. J. Robinson and P. M. Maitlis, *J. Organomet. Chem.*, 1985, **279**, 115; (*d*) G. J. Sunley, P.del C. Menanteau, H. Adams, N. A. Bailey and P. M. Maitlis, *J. Chem. Soc., Dalton Trans.*, 1989, 2415; (*e*) N. Dudeney, O. N. Kirchner, J. C. Green and P. M. Maitlis, *J. Chem. Soc., Dalton Trans.*, 1984, 1877; (*f*) M. Gomez, J. M. Kisenyi, G. J. Sunley and P. M. Maitlis, *J. Organomet. Chem.*, 1985, **296**, 197; (*g*) F. P. Fanizzi, G. J. Sunley, J. A. Wheeler, H. Adams, N. A. Bailey and P. M. Maitlis, *Organometallics*, 1990, **9**, 131.

10 Experimental conditions: 2.0 mM substrate in Me_2SO/0.1 M $Bu_4N^+PF_6^-$, 25 °C $d = 0.4$ mm Pt disk electrode.

11 A. J. Bard and L. R. Faulkner, *Electrochemical Methods. Fundamentals and Applications*, Wiley, New York, 1980.

12 The change of supporting electrolyte compared to that used for the CV investigation was done in order to facilitate the separation of product and electrolyte during work-up, see the Experimental section for details.

13 In these measurements a faint, but fairly constant current was observed to flow through the cell well after the consumption of 1 Faraday mol^{-1} and after unusually long electrolysis times. Similar behavior has been reported by others and has been attributed to the generation of species that are capable of mediating electrocatalytic solvent oxidation, see G. S. Bodner, J. A. Gladysz, M. F. Nielsen and V. D. Parker, *Organometallics*, 1987, **6**, 1628.

14 (*a*) M. Tilset, in *Energetics of Organometallic Species*, ed. J. A. M. Simões, Kluwer Academic, Dordrecht, 1992, p. 109; (*b*) M. Tilset, V. Skagestad and V. D. Parker, in *Molecular Electrochemistry of Inorganic, Bioinorganic and Organometallic Compounds*, eds. A. J. L. Pombeiro and J. A. McCleverty, Kluwer Academic, Dordrecht, 1992, p. 267.

15 Uncertainties in activation parameters are given as two standard deviations from the regression analysis.

16 N. G. Connelly and W. E. Geiger, *Chem. Rev.*, 1996, **96**, 877.

17 Isotopomer distribution was determined by comparison of the mass spectrum of the experimental isotopomer mixture to peak intensities in reference spectra of the individual isotopomers: C_2H_4 (53–98%), C_2D_4 (1–40%), C_2H_3D (0–29%), $C_2H_2D_2$ (0–2%), C_2HD_3 (0–15%).

18 Approximate H_2O content of 0.6 mol% was estimated by comparison of NMR integrals of water and residual protio-dimethylsulfoxide in the deuterated solvent.

19 For some pertinent reviews, see: (*a*) D. Astruc, *Electron Transfer and Radical Processes in Transition-Metal Chemistry*, VCH, Weinheim, 1995; (*b*) D. Astruc, *Organometallic Radical Processes*, ed. W. C. Trogler, Elsevier, Amsterdam, 1990.

20 P. M. Maitlis, *Chem. Soc. Rev.*, 1981, **10**, 1.

21 M. Tilset, G. S. Bodner, D. R. Senn, J. A. Gladysz and V. D. Parker, *J. Am. Chem. Soc.*, 1987, **109**, 7551.

22 C. White, A. J. Oliver and P. M. Maitlis, *J. Chem. Soc., Dalton Trans.*, 1973, 1901; A. Vázquez de Miguel, K. Isobe, B. F. Taylor, A. Nutton and P. M. Maitlis, *J. Chem. Soc., Chem. Commun.*, 1982, 758.

23 F. W. B. Einstein, R. H. Jones, X. Zhang, X. Yan, R. Nagelkerke and D. Sutton, *J. Chem. Soc., Chem. Commun.*, 1989, 1424.

24 A. C. Cope, *J. Am. Chem. Soc.*, 1935, **57**, 2238.

25 R. G. Ball, W. A. G. Graham, D. M. Heinekey, J. K. Hoyano, A. D. McMaster, B. M. Mattson and S. T. Michel, *Inorg. Chem.*, 1990, **29**, 2023.

26 M. Brookhart, B. Grant and A. F. Volpe, *Organometallics*, 1992, **11**, 3920.

27 M. N. Burnett and C. K. Johnson, ORTEP3, Report ORNL-6895, Oak Ridge National Laboratory, Oak Ridge, TN, 1996.